The kinetochore protein Ndc10p is required for spindle stability and cytokinesis in yeast

David C. Bouck and Kerry S. Bloom*

Department of Biology, University of North Carolina, Chapel Hill, NC 27599

Edited by Ronald D. Vale, University of California, San Francisco, CA, and approved March 7, 2005 (received for review August 12, 2004)

The budding yeast kinetochore is comprised of >60 proteins and associates with 120 bp of centromeric (CEN) DNA. Kinetochore proteins are highly dynamic and exhibit programmed cell cycle changes in localization. The CEN-specific histone, Cse4p, is one of a few stable kinetochore components and remains associated with CEN DNA throughout mitosis. In contrast, several other kinetochore proteins have been observed along interpolar microtubules and at the midzone during anaphase. The inner kinetochore protein, Ndc10p, is enriched at the spindle midzone in late anaphase. We show that Ndc10p is transported to the plus-ends of interpolar microtubules at the midzone during anaphase, a process that requires survivin (Bir1p), a member of the aurora kinase (Ipl1p) complex, and Cdc14p phosphatase. In addition, Ndc10p is required for essential non-kinetochore processes during mitosis. Cells lacking functional Ndc10p show defects in spindle stability during anaphase and failure to split the septin ring during cytokinesis. This latter phenotype leads to a cell separation defect in *ndc10–1* cells. We propose that Ndc10p plays a direct role in maintaining spindle stability during anaphase and coordinates the completion of cell division after chromosome segregation.

microtubule | survivin | mitosis | septin

Mitosis is the process of segregating equal complements of the replicated genome to daughter cells before cytokinesis. Successful chromosome segregation requires the temporal regulation of sister chromatid biorientation, anaphase onset, spindle disassembly, and cytokinesis. Chromosomes are tethered to microtubules of the mitotic spindle by multiprotein, centromere (CEN)-associated complexes known as kinetochores. The kinetochore functions to capture microtubules, maintain attachment to growing and shortening microtubule plus-ends under tension, provide a framework for the spindle assembly checkpoint, and promote microtubule plus-end depolymerization at anaphase onset. Upon anaphase onset, chromosomal passenger proteins relocalize from the CEN to the spindle midzone, where they are proposed to play roles in spindle stability, timing of spindle disassembly, and cytokinesis (1, 2).

Despite its relatively simple CEN, the budding yeast kinetochore is comprised of at least 60 proteins that assemble into discrete subcomplexes (3). A functional kinetochore minimally requires a CEN-specific binding complex, a microtubule-binding complex, and regulatory/checkpoint complexes, which ensure the accuracy of attachments (4). Biochemical and genetic analyses of the kinetochore have shown that the CEN-binding factor 3 (CBF3) complex, comprised of Ndc10p, Cep3p, Ctf13p, and Skp1p, specifically binds CEN DNA (5, 6). The Dam1 complex is proposed to associate directly with microtubules (7–10). Regulation of kinetochore attachment to microtubules is likely mediated by the Ipl1p–Bir1p–Sli15p complex (IBS) under surveillance of the spindle assembly checkpoint (11–14). The functions of other kinetochore subcomplexes and their individual proteins remain to be understood.

The labeling of kinetochore proteins with GFP has enabled the characterization of kinetochore–CEN complexes in living cells. In G_1, unreplicated kinetochores remain closely tethered to the spindle pole body (SPB) (15). Coincident with or shortly after DNA replication, kinetochores establish attachments to one of the duplicated SPBs. Chromatids of the same replicative age are randomized between SPBs, indicating that old kinetochore–pole attachments are labile, and new attachments are promoted to both old and new poles (16). It has been proposed that the aurora kinase Ipl1p promotes kinetochore–microtubule detachment (13). In this way, errors in attachment are continually corrected through detachment/attachment cycles until tension among sister chromatids is attained.

In G_2/M, the sister chromatids have bioriented, and kinetochore complexes appear as two clusters along the spindle axis (17). Fluorescent labeling of individual chromosomes near the CEN has revealed that individual kinetochore–CEN complexes oscillate along the spindle until anaphase onset (17–21). Anaphase includes the movement of kinetochores to their respective SPBs in anaphase A and the elongation of polymerizing interpolar spindle microtubules (anaphase B) until the spindle extends across the length of the budded cell (20). The anaphase spindle remains intact until the genomes are completely segregated.

During early anaphase, Cdc14p is activated and freed from the nucleolus. Cdc14p phosphatase activity leads to the dephosphorylation of the yeast INCENP Sli15p, resulting in the localization of Sli15, Ipl1p, and the kinetochore protein Slk19p to the midzone (22). The budding yeast midzone consists of overlapping antiparallel microtubule plus-ends (23, 24). Slk19p and Sli15p have been proposed to contribute to anaphase spindle stability, whereas Ipl1p has been proposed to regulate the timing of spindle disassembly (2, 22, 25).

Completion of the budding yeast cell cycle is marked by cytokinesis and the separation of daughter cells (26). These processes are initiated by the organization of septins at the bud neck, where they form a ring. The septin ring splits into two rings before constriction of the actomyosin ring and forms compartments that retain cortical factors necessary for neck constriction, membrane addition, and cell wall synthesis (27, 28). Division of the cytoplasm is followed by the physical separation of the adjoining cells through septum abscission.

In this work, we have used high-resolution time-lapse microscopy to examine the dynamic localization of members of the major kinetochore subcomplexes throughout the cell cycle and characterized their non-CEN localization. Kinetochore proteins follow four distinct localization patterns during anaphase spindle elongation. We have focused our study on the inner kinetochore protein Ndc10p, a member of the CBF3 complex that localizes to both CEN DNA and the spindle midzone during anaphase (25, 29). Ndc10p associates with the plus-ends of interpolar microtubules during spindle disassembly and continues to associate with nonkinetochore microtubules during telophase. This CEN DNA-independent association of Ndc10p with microtu-

This paper was submitted directly (Track II) to the PNAS office.

Abbreviations: SPB, spindle pole body; CEN, centromere; IBS, Ipl1p-Bir1p-Sli15p complex; CBF3, centromere-binding factor 3.

*To whom correspondence should be addressed. E-mail: kerry_bloom@unc.edu.

www.pnas.org/cgi/doi/10.1073/pnas.0405925102

bules requires Cdc14p and the budding yeast survivin homolog Bir1p. We have also examined novel *ndc10* phenotypes and found that *ndc10–1* cells exhibit spindle stability defects during anaphase spindle elongation. Additionally, *ndc10–1* cells fail to properly organize septins at the bud neck and show defects in the last step of the budding yeast cell cycle, cell separation.

Materials and Methods

Yeast Strains and Media. All strains used are listed in Table 1, which is published as supporting information on the PNAS web site, and were constructed in the YEF473A background (unless otherwise noted) by using previously described techniques (see *Supporting Text*, which is published as supporting information on the PNAS web site) (30).

Cells were grown in rich or selective media, as appropriate. Azide treatment was carried out as described (31). G_1 arrest was induced with 15 μg/ml α-factor.

Image Acquisition and Presentation. Images were acquired on a Nikon E600FN microscope by using a 100× 1.4-numerical aperture objective. Further details of techniques and equipment used in image acquisition have been discussed elsewhere (see *Supporting Text*) (32).

Z-series stacks were compiled by maximum projection for presentation (32). Kymographs were created by drawing an 8- by 10-pixel-wide line across the spindle as described (23).

Z-series compilations, kymographs, distance, and fluorescence intensity measurements were carried out with METAMORPH software (Universal Imaging, Downingtown, PA). When necessary, data were exported to Microsoft EXCEL 2000 for calculations and graphing. Images were arranged with COREL-DRAW 10 (Corel, Ottawa, ON, Canada).

Examination of *ndc10–1* Phenotypes. To examine spindle defects, wild-type and *ndc10–1* cells expressing GFP-Tub1p were grown to log phase at 24°C and then treated for 3 h with α-factor (15 μg/ml) to synchronize cells in G_1. Cells were shifted to 37°C for an additional 30 min before release. Cells were washed three times to remove α-factor and grown at 37°C. Samples were collected at 20-min intervals and fixed for 30 min in 3.7% formaldehyde at room temperature. Spindles were measured and categorized according to their length and morphology. Cells that had not yet formed bipolar spindles were classified as monopolar. Bipolar spindles <3 μm were classified as short spindles, 3- to 6-μm bipolar spindles as medium, and >6-μm spindles as long. Broken/disassembled spindles were defined as those that had one SPB in both the mother and bud but were no longer linked to each other by visible interpolar microtubules.

To examine cytokinetic/cell separation defects, wild-type and *ndc10–1* cells were grown to log phase at 24°C and then treated for 3 h with α-factor (15 μg/ml). Cells were shifted to 37°C for an additional 30 min before being washed three times to release them from arrest. *GAL-UB-NUF2 mad2*Δ cells were arrested in galactose medium using α-factor. After 3 h, glucose was added to 2%, and cells were incubated for 1 h. Cells were then washed three times and released into glucose medium. After 3–4 h from release, cells were briefly sonicated before imaging. Mother cells with more than one daughter bud attached were scored as multibudded.

Lytic digestion of *ndc10–1* cells was adapted from previous work (33, 34). Cells were fixed for 60 min at room temperature in 3.7% formaldehyde and then washed into 1 M sorbitol. Lyticase was added to a final concentration of 80 units/ml, and cells were incubated at 37°C for 60 min before imaging.

Results

Kinetochore Proteins Are Highly Dynamic and Exhibit Programmed Cell Cycle Changes in Localization. Cse4p, the budding yeast CENP-A homologue, and Nuf2p, an essential kinetochore protein involved in checkpoint monitoring of the kinetochore (35, 36), form two foci that represent clusters of separated sister CENs in metaphase (37). These foci segregate to opposite SPBs during anaphase and remain proximal to the SPBs into the next cell cycle (Fig. 1*A*; data not shown). Cse4p-GFP and Nuf2p-GFP are not detectable at other structures in the cell (Fig. 1*A*; data not shown). This behavior reflects the CEN DNA position, as demonstrated by using the lacO-lacI-GFP-labeling method (17–20).

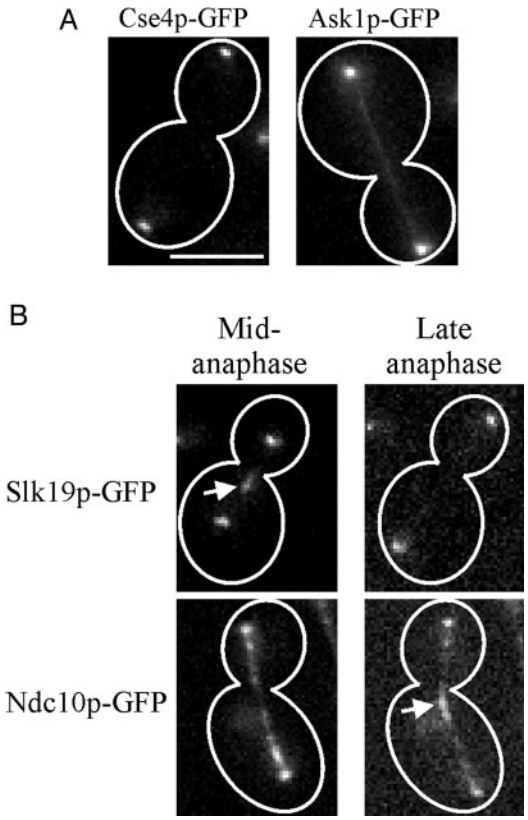

Fig. 1. Anaphase localization of kinetochore proteins exhibits four distinct classes. Selected frames from time-lapse observation of live cells expressing Cse4p-GFP, Ask1p-GFP, Slk19p-GFP, or Ndc10p-GFP. (*A*) Cse4p-GFP is detectable only as two bright kinetochore clusters. Ask1p-GFP remains bound along microtubules and at kinetochores. (*B*) Slk19p-GFP localizes to kinetochores and the midzone (arrow), but the midzone signal decreases as anaphase proceeds. Ndc10p-GFP localizes along the spindle in anaphase and is enriched at the midzone (arrow) before spindle disassembly. (Bar, 5 μm.)

A second class of kinetochore protein decorates the kinetochore and microtubules. In anaphase, Ask1p-GFP (a member of the Dam1 complex) forms two kinetochore foci, in addition to its distribution along interpolar microtubules throughout spindle elongation and disassembly (Fig. 1*A* and data not shown). The association of Ask1p-GFP along microtubules is consistent with the recent finding that the Dam1 complex forms ring-like structures around microtubules *in vitro* (9, 10). Other members of the Dam1 complex form kinetochore foci and localize along the anaphase spindle (7, 8) (data not shown).

Among the microtubule-associated kinetochore proteins, several accumulate at the spindle midzone with quantitative differences in timing and persistence. The accessory kinetochore protein Slk19p-GFP can be found in two kinetochore foci in metaphase. Shortly after anaphase onset, Slk19p migrates to the midzone, whereupon it dissociates as anaphase elongation progresses (Fig. 1*B* and Fig. 7*A*, which is published as supporting information on the PNAS web site). Fluorescence intensity

CELL BIOLOGY

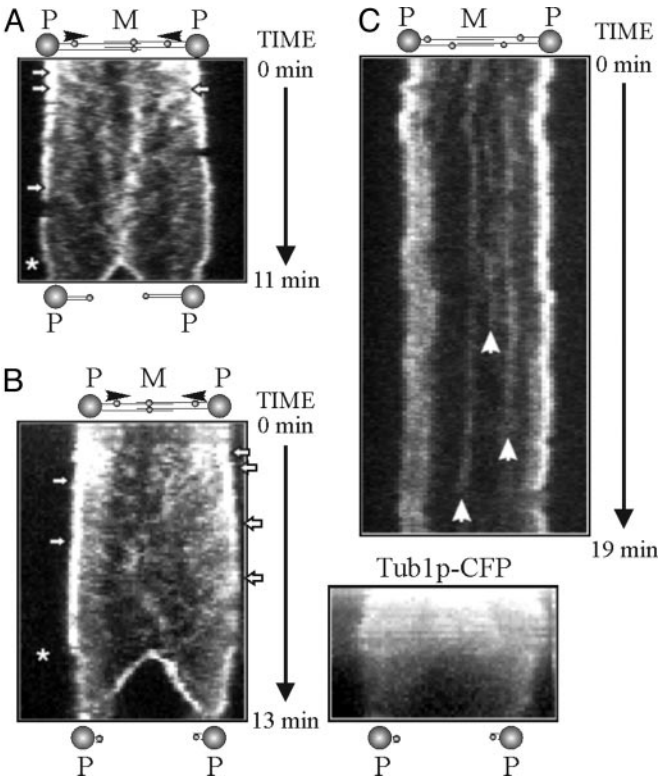

Fig. 2. Dynamic translocation of Ndc10p-GFP to the anaphase spindle midzone. (*A*) Kymograph of Ndc10p-GFP in a late anaphase spindle shows movement toward the midzone. The kymograph shows movement along the spindle through time. Vertical lines represent static foci, whereas movement is shown as sloped lines (arrows indicate instances of movement toward the midzone). (*B*) Midzone Ndc10p-GFP tracks the plus-ends of the depolymerizing interpolar microtubules during spindle disassembly (asterisk marks start of spindle disassembly). CFP-Tub1p indicates spindle disassembly is coincident with the movement of midzone Ndc10p-GFP to the SPBs. (*C*) Sodium azide treatment of cells inhibits the translocation of Ndc10p-GFP along anaphase spindle. Arrows indicate static Ndc10p-GFP foci along the anaphase spindle.

measurements of Slk19p-GFP at the midzone and kinetochores during anaphase progression show that Slk19p-GFP signal intensity decays more rapidly at the midzone than at the kinetochores (Fig. 7*B*). By late anaphase, Slk19p-GFP is no longer detectable at the spindle midzone (Fig. 1*B*).

The localization of several kinetochore components, including Ndc10p, the aurora kinase Ipl1p, and Sli15p, resembles passenger proteins observed in higher eukaryotes (38). Ndc10p forms two kinetochore foci before anaphase (39). Shortly after anaphase onset (≈4 min), a fraction of Ndc10p-GFP associates with the spindle and is eventually translocated to the spindle midzone in late anaphase, where it forms a cluster at the plus-ends of interpolar microtubules (Fig. 1*B*; Movie 1, which is published as supporting information on the PNAS web site). CEN-bound kinetochores remain adjacent to the SPB in late anaphase, thus the Ndc10p fraction at the midzone reflects the CEN-independent microtubule association of this protein. Treatment of cells with sodium azide inhibited the translocation of Ndc10p to the spindle midzone, suggesting that this movement is an ATP-driven process (compare Fig. 2 *A* and *C*). Upon spindle disassembly, the microtubule plus-ends depolymerize, and midzone Ndc10p-GFP breaks into two foci that migrate with the shortening microtubule plus-ends to their respective poles (Fig. 2*B*, asterisk). These two Ndc10p-GFP foci migrate with an average velocity of 2 μm/min to their respective SPBs. Thus,

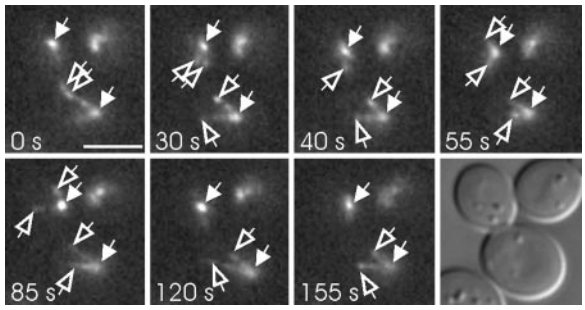

Fig. 3. Ndc10p-GFP localizes with growing and shortening microtubules. Time lapse of a late anaphase cell expressing Ndc10p-GFP. At first timepoint, spindle disassembly has just begun, and midzone Ndc10p-GFP has broken into two clusters (hollow arrowheads). As these clusters follow the plus-ends of depolymerizing microtubules, other projections of Ndc10p-GFP grow and shrink from the region of the SPB (white arrows). (Bar, 5 μm.)

Ndc10p accumulates at the spindle midzone as anaphase progresses and associates with microtubule plus-ends.

Ndc10p-GFP Localizes to Growing and Shrinking Microtubules. During spindle disassembly in telophase and G_1 of the next cell cycle, we observed Ndc10p-GFP along projections extending from the SPBs. These projections were dynamic (making poleward and antipoleward movements), suggesting that Ndc10p-GFP is localizing along growing and shrinking nuclear microtubules in telophase (Fig. 3; Movie 2, which is published as supporting information on the PNAS web site). The rates of growth and shortening were 2.4 and 1.1 μm/min, respectively, within the range of previous estimates of cytoplasmic microtubule growth and shortening (40, 41).

Translocation of the Inner Kinetochore Complex CBF3 to the Midzone Requires Cdc14p and Survivin (Bir1p). The CEN-binding CBF3 complex, including Ndc10p, exhibits DNA sequence specificity but no direct microtubule binding (42). Therefore, we considered that Ndc10p translocation could depend upon one of the midzone complexes, including IBS. Ndc10p, and Bir1p, were previously identified as interaction partners in a two-hybrid screen, and Ndc10p is an *in vitro* substrate of the aurora kinase, Ipl1p (12, 43). To test whether Ndc10p localization to the midzone depends on Bir1p, we examined the localization of Ndc10p-GFP in cells lacking Bir1p (using a temperature degron *BIR1* allele, *bir1*^{td}; see *Supporting Text*). In wild-type cells, Ndc10p-GFP forms foci adjacent to SPBs and along the spindle in late anaphase (Fig. 4*A*). In Bir1p-depleted cells, Ndc10p-GFP failed to localize along the spindle during anaphase (Fig. 4*A*). In late anaphase, Ndc10p-GFP formed two kinetochore foci (located adjacent to the SPBs) but failed to localize to the spindle midzone. In contrast, Ndc10p-GFP localized along the anaphase spindle at only slightly lower levels in *ipl1–321* cells (Fig. 4*B*), suggesting that Bir1p plays a direct role in the association of Ndc10p with interpolar microtubules.

The localization of Ndc10p along the anaphase spindle and to interpolar microtubule plus-ends could be unique to Ndc10p or could indicate novel localization of the entire CBF3 complex. Ctf13p, the core of the CBF3 complex, binds dimers of Ndc10p and Cep3p to form CBF3 (44). Cep3p-GFP formed two kinetochore clusters in metaphase that migrated to opposite poles at anaphase onset (data not shown). Like Ndc10p-GFP, Cep3p-GFP localized along the anaphase spindle, enriched at the midzone, and separated into two foci that moved poleward during spindle disassembly (Fig. 4*A*; data not shown). However, in *bir1*^{td} cells, Cep3p-GFP failed to localize to the anaphase spindle or midzone (Fig. 4*A*). These results suggest that the

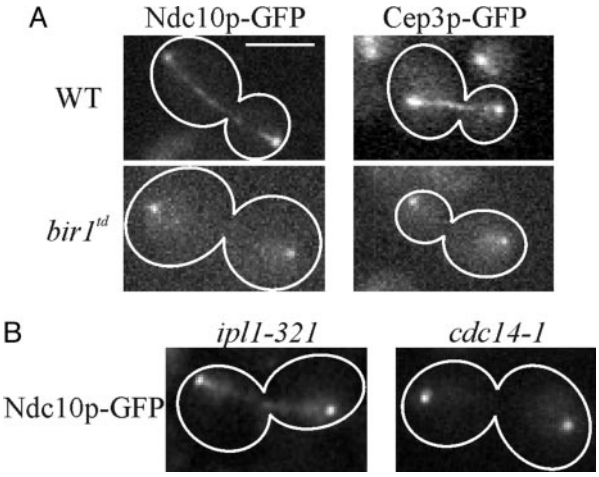

Fig. 4. CBF3 association with the anaphase spindle requires Bir1p and Cdc14p. (*A*) Localization of two CBF3 components, Cep3p and Ndc10p, in wild-type cells shows localization along the anaphase spindle. Loss of Bir1p, by using a temperature-degron allele of *BIR1* (see *Material and Methods*), results in loss of CBF3 association with interpolar microtubules and the spindle midzone. (*B*) Ndc10p-GFP localization in *ipl1–321* and *cdc14–1* cells grown under nonpermissive conditions. (Bar, 5 μm.)

entire CBF3 complex localizes to interpolar microtubules during anaphase, and that the CBF3 complex associates with interpolar microtubules in a Bir1p-dependent manner.

The redistribution of CBF3 to interpolar microtubules coincides with the release of the Cdc14 phosphatase from the nucleolus and spindle microtubule stability upon anaphase onset (45). In addition, the accumulation of IBS to the midzone depends on Cdc14p activity (22). Ndc10p-GFP failed to localize to the anaphase spindle in *cdc14–1* cells grown at 37°C, indicating that the midzone localization of CBF3, like IBS, depends on Cdc14p (Fig. 4*B*).

Ndc10p Is Required for Spindle Stability During Anaphase. In wild-type cells, the anaphase spindle elongates $\approx$10 μm, the full length of the budded cell before disassembly. To test whether *ndc10–1* cells have defects in spindle elongation, we examined spindle length and morphology in wild-type and *ndc10–1* cells synchronized in G_1 and released at 37°C (Fig. 5 *A* and *B*; see *Material and Methods*). After 60 min from release, most wild-type cells had formed bipolar spindles, and nearly half (45%) had long spindles characteristic of late anaphase. By 80 min, 72% of cells had disassembled spindles, indicative of telophase. In contrast, after 60 min from release, 11% of *ndc10–1* cells had long spindles, whereas most had either short- (38%) or medium- (39%) length spindles. At no timepoint did >11% of *ndc10–1* cells have long spindles. Cells lacking functional Ndc10p form preanaphase bipolar spindles, but these spindles fail to fully elongate during anaphase.

Time-lapse imaging of spindles in *ndc10–1* cells grown at restrictive temperature revealed cycles of partial elongation and collapse, without full elongation along the mother-bud axis (Fig. 5 *C* and *D*). These cycles of failed spindle elongation support the finding that anaphase spindle stability requires functional Ndc10p.

Spindle elongation defects in *ndc10–1* cells might be a consequence of loss of kinetochore function, rather than loss of Ndc10p function. To explore this possibility, kinetochore function was disrupted by placing the kinetochore component Nuf2p under control of the inducible *GAL1* promoter. In addition, the spindle checkpoint gene *MAD2* was deleted to allow anaphase progression in the absence of a kinetochore. This strain showed

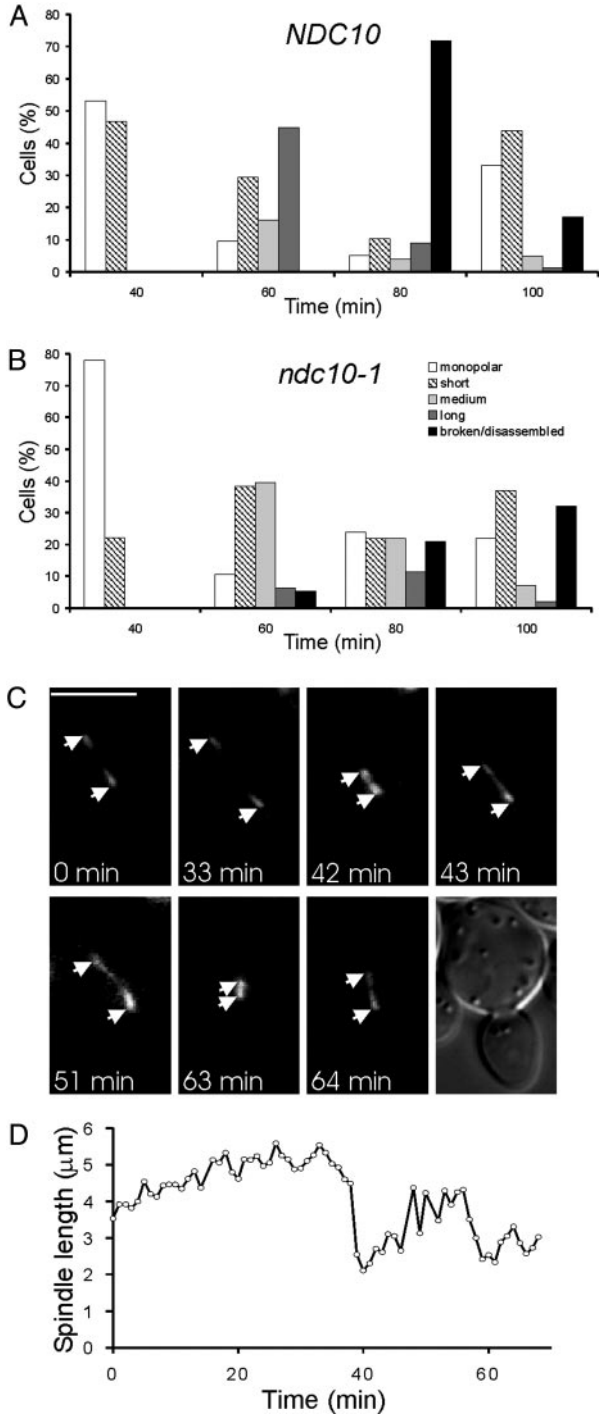

Fig. 5. Ndc10p is required for spindle stability during anaphase and cell separation. Wild-type and *ndc10–1* cells were arrested in G_1 with α-factor and released at 37°C. Spindles were categorized as being monopolar, short, medium, long, or broken/disassembled based on morphology and length of GFP-Tub1p fluorescence (see *Materials and Methods*). (*A*) Spindle lengths of wild-type cells released from G_1 arrest at 37°C. (*B*) Spindle lengths of *ndc10–1* cells released from G_1 arrest at 37°C. (*C*) Time-lapse fluorescence images of GFP-Tub1p in *ndc10–1* cells grown at 37°C. (Bar, 5 μm.) (*D*) Quantitation of spindle length for cell presented in *C*.

no defects in the formation of long spindles after Nuf2p depletion (Fig. 8, which is published as supporting information on the PNAS web site). Thus functional Ndc10p, and not the kinetochore, is required for the stability of elongating spindles.

CELL BIOLOGY

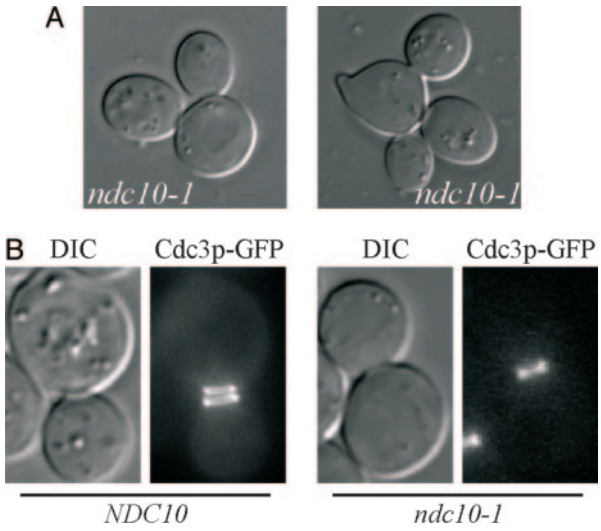

Fig. 6. Cell-separation defects in ndc10–1 cells. (*A*) *ndc10–1* cells grown at 37°C for 3–4 h form multicell clusters. (*B*) Fluorescence images of the septin Cdc3p-GFP in wild-type and *ndc10–1* cells. In wild-type cells, Cdc3p-GFP splits into two rings at the time of cytokinesis, but in *ndc10–1* cells, the septin ring fails to divide.

***ndc10–1* Cells Exhibit Defects in Cytokinesis and Cell Separation.** Passenger proteins have been postulated to contribute to cytokinesis in tissue cells. To determine whether Ndc10p exhibits similar function at spindle microtubule plus-ends in anaphase, we examined the terminal cell morphology of *ndc10–1* cells. Cells were released from G_1 arrest and grown for 3–4 h at 24 or 37°C. Although *ndc10–1* cells grown at permissive temperature showed no unusual cell morphology (0 of 100 cells were multibudded), 83% of *ndc10–1* cells at 37°C had multiple buds attached to the same mother ($n = 100$; Fig. 6*A*). Wild-type cells grown at 37°C showed no unusual morphology (3% multibudded; $n = 100$). The multibudded phenotype is indicative of multiple cell cycles in the absence of division. Thus, *ndc10–1* cells fail to complete cell division.

To explore this defect in cell division, we examined the localization of the septin Cdc3p in *ndc10–1* cells. In wild-type cells, the septin ring splits into two at the bud neck before constriction of the actomyosin ring (Fig. 6*B*). In *ndc10–1* cells, Cdc3p-GFP localized to the neck as a single ring but failed to split ($n = 60$; Fig. 6*B*). This defect in septin organization indicates that Ndc10p is required for a critical step at the end of the cell cycle.

Multibudded cells could arise from defects in cytokinesis or the physical separation of the adjoining cells through the degradation of the septum. To determine whether Ndc10p is required for cytokinesis or cell separation, *ndc10–1* cells were fixed and digested with lyticase. This treatment results in the declustering of multibudded cells defective in cell separation, whereas cells that have failed to undergo cytokinesis remain clustered (33, 34). Multibudded *myo1*Δ cell clusters, which have a defect in cell separation, dissociated after digestion, whereas *cdc14–1* cells, which arrest in late anaphase (before cytokinesis), remained clustered (Fig. 9, which is published as supporting information on the PNAS web site) (34, 46). We found that lyticase treatment of *ndc10–1* cells released the cell clusters, indicating that *ndc10–1* cells undergo cytokinesis but not cell separation (Fig. 9).

The multibudded phenotype seen in *ndc10–1* cells is similar to the morphology of spindle checkpoint mutants treated with microtubule depolymerizing agents (47, 48). *NDC10* has also been reported to be essential for spindle checkpoint activation (49). Together, these observations suggest that the multibudding seen in *ndc10–1* cells might be an effect of the loss of kinetochore–microtubule attachment in a checkpoint-deficient background. To examine the possibility that other kinetochore defects in a checkpoint-deficient strain could lead to multibudding, we examined the morphology of *GAL1-UB-NUF2 mad2*Δ cells after 4 h of *NUF2* repression in glucose-containing medium. Depletion of Nuf2p in a spindle checkpoint-deficient strain did not result in multibud phenotype (data not shown), suggesting that Ndc10p, and not the kinetochore, is essential for successful cell separation.

Discussion

We have demonstrated that the major CEN–DNA-binding complex (CBF3) accumulates at the spindle midzone during anaphase and along growing and shrinking microtubule plus-ends in telophase and G_1 (Figs. 2 and 3). Studies of CBF3 have focused on its role in kinetochore formation at CEN DNA. The finding that CBF3 localizes to microtubule plus-ends reveals critical roles for CBF3 in stabilizing the anaphase spindle and ensuring that cytokinesis follows chromosome segregation to the spindle poles.

Ndc10p Stabilizes the Anaphase Spindle. In the absence of functional Ndc10p, the spindle fails to fully elongate during anaphase (Fig. 5). Spindle elongation was not compromised in strains lacking kinetochores (*GAL1-UB NUF2*) (Fig. 8). Thus Ndc10p is specifically required for spindle stability. Ndc10p association with the anaphase spindle depends on the Cdc14p phosphatase that has recently been shown to dampen anaphase spindle microtubule dynamics (Fig. 4*B*) (45). Additionally, microtubule dynamics are regulated primarily at the plus-end in budding yeast (23). These findings indicate that Cdc14p-dependent release of Ndc10p to microtubule plus-ends may contribute to microtubule stability in the anaphase spindle. We found that spindles in *ndc10–1* cells collapsed by the 5- to 6-μm stage of spindle elongation, when there are relatively few interpolar microtubules (less than four per SPB). Anaphase spindle elongation provides the motive force for chromosome segregation in yeast. It is therefore critical that the spindle midzone remain intact during anaphase spindle elongation.

Ndc10p Is Required for Completion of Cell Division. The accumulation of multibudded cells in *ndc10–1* mutants indicates that Ndc10p is required for cell separation before entry into the next cell cycle (Fig. 6*A*). The multibudded phenotype is similar to *mad1,2,3* and *bub1,2,3* mutants treated with microtubule depolymerizing agents (47, 48). In the absence of the spindle checkpoint, cells attempt to reenter the cell cycle despite their inability to maintain a mitotic spindle. Likewise, in *ndc10–1* cells, spindle checkpoint function is lost, and spindle structure is compromised, suggesting the importance of both checkpoint function and spindle integrity for completion of cell division and regulated entry into the next cell cycle. However, the lack of multibudded cells upon depletion of Nuf2p indicates that Ndc10p, and not the kinetochore itself, is essential for cell separation.

The failure to complete cell division in *ndc10–1* cells was confirmed by the altered organization of septins in these cells. Examination of the Cdc3p-GFP localization in *ndc10–1* cells revealed a failure of the septin ring to divide into two rings during cytokinesis (Fig. 6*B*). The septins are thought to recruit and/or maintain the exocytic machinery involved in secretion at the bud neck (28). Failure to split the septin rings would presumably result in defects during cytokinesis. However, the terminal morphological phenotype of *ndc10–1* cells is a failure to separate cells rather than complete cytokinesis (as assayed by cell cluster dispersion after enzymatic digestion of the cell wall).

This suggests that the septin defect in *ndc10–1* cells might cause a malformed septum during cytokinesis, resulting in a structure that cannot be dissolved during cell separation.

In higher eukaryotes, the spindle midzone and the delivery of passenger proteins to microtubule plus-ends appear to be essential for proper cytokinesis (50). Furthermore, the requirement of Ndc10p for cytokinesis provides a mechanism that ensures chromosome segregation to the poles before cytokinesis. The key regulatory step could be the release of Ndc10p to the midzone upon anaphase onset.

Nonkinetochore CBF3 Forms a "Prekinetochore?" The localization of CBF3 to nonkinetochore microtubules is evident from telophase and persists into G_1 of the next cell cycle. Ndc10p localizes to both growing and shortening microtubules emanating from the SPB (Fig. 3). This behavior is reminiscent of microtubule "search-and-capture" mechanisms that facilitate the establishment of kinetochore–microtubule attachments in tissue cells. CEN DNA is replicated early in S phase, and sister chromatid biorientation can occur before the completion of DNA replication (17, 51). Thus, early in the cell cycle, kinetochore–microtubule attachments can be made. These "prekinetochores" are likely to contain the IBS complex, because Bir1p is required for Ndc10p plus-end localization. IBS promotes biorientation of sister kinetochores during search and capture by promoting kinetochore–microtubule detachment until tension is attained (13). These prekinetochores could mature into functional kinetochores upon CEN DNA binding and the recruitment of the additional kinetochore complexes, which would confer stability and checkpoint function to the structure. The essential functions of kinetochores are CEN DNA binding and association with dynamic microtubule plus-ends. CBF3 was first identified as a CEN-binding complex, and more recently Ndc10p has been localized along microtubules of both long and short spindles (5, 29). Our data reveal that CBF3 associates with both growing and shrinking microtubules independent of CEN DNA, and Ndc10p provides critical functions in spindle stability and cytokinesis.

We thank J. Molk, C. Pearson, N. Ko, and J. Pringle for helpful discussions and technical assistance; E. Yeh and K. Mythreye for critical reading of the manuscript; and R. Heil-Chapdeleine (Washington University, St. Louis, MO), J. Cooper (Washington University, St. Louis, MO), M. Fitzgerald-Hayes (University of Massachusetts, Amherst), W. Saunders (University of Pittsburgh, Pittsburgh), I. Cheeseman (University of California, Berkeley), G. Barnes (University of California, Berkeley), C. Caruso (University of North Carolina, Chapel Hill), J. Pringle (University of North Carolina, Chapel Hill), and S. Biggins (Fred Hutchinson Cancer Research Center, Seattle) for strains and plasmids. This work was supported by National Institutes of Health Grant GM-32238 (to K.S.B.).

1. Adams, R. R., Carmena, M. & Earnshaw, W. C. (2001) *Trends Cell Biol.* **11,** 49–54.
2. Buvelot, S., Tatsutani, S. Y., Vermaak, D. & Biggins, S. (2003) *J. Cell Biol.* **160,** 329–339.
3. McAinsh, A. D., Tytell, J. D. & Sorger, P. K. (2003) *Annu. Rev. Cell Dev. Biol.* **19,** 519–539.
4. Rieder, C. L. & Salmon, E. D. (1998) *Trends Cell Biol.* **8,** 310–318.
5. Lechner, J. & Carbon, J. (1991) *Cell* **64,** 717–725.
6. Connelly, C. & Hieter, P. (1996) *Cell* **86,** 275–285.
7. Li, Y., Bachant, J., Alcasabas, A. A., Wang, Y., Qin, J. & Elledge, S. J. (2002) *Genes Dev.* **16,** 183–197.
8. Cheeseman, I. M., Brew, C., Wolyniak, M., Desai, A., Anderson, S., Muster, N., Yates, J. R., Huffaker, T. C., Drubin, D. G. & Barnes, G. (2001) *J. Cell Biol.* **155,** 1137–1145.
9. Westermann, S., Avila-Sakar, A., Wang, H. W., Niederstrasser, H., Wong, J., Drubin, D. G., Nogales, E. & Barnes, G. (2005) *Mol. Cell* **17,** 277–290.
10. Miranda, J. J., De Wulf, P., Sorger, P.K. & Harrison, S. C. (2005) *Nat. Struct. Mol. Biol.* **12,** 138–143.
11. Cheeseman, I. M., Anderson, S., Jwa, M., Green, E. M., Kang, J., Yates, J. R., III, Chan, C. S., Drubin, D. G. & Barnes, G. (2002) *Cell* **111,** 163–172.
12. Biggins, S., Severin, F. F., Bhalla, N., Sassoon, I., Hyman, A. A. & Murray, A. W. (1999) *Genes Dev.* **13,** 532–544.
13. Tanaka, T. U., Rachidi, N., Janke, C., Pereira, G., Galova, M., Schiebel, E., Stark, M. J. & Nasmyth, K. (2002) *Cell* **108,** 317–329.
14. Lew, D. J. & Burke, D. J. (2003) *Annu. Rev. Genet.* **37,** 251–282.
15. Jin, Q. W., Fuchs, J. & Loidl, J. (2000) *J. Cell Sci.* **113,** 1903–1912.
16. Neff, M. W. & Burke, D. J. (1991) *Genetics* **127,** 463–473.
17. Goshima, G. & Yanagida, M. (2000) *Cell* **100,** 619–633.
18. Straight, A. F., Marshall, W. F., Sedat, J. W. & Murray, A. W. (1997) *Science* **277,** 574–578.
19. He, X., Asthana, S. & Sorger, P. K. (2000) *Cell* **101,** 763–775.
20. Pearson, C. G., Maddox, P. S., Salmon, E. D. & Bloom, K. (2001) *J. Cell Biol.* **152,** 1255–1266.
21. Tanaka, T., Fuchs, J., Loidl, J. & Nasmyth, K. (2000) *Nat. Cell Biol.* **2,** 492–499.
22. Pereira, G. & Schiebel, E. (2003) *Science* **302,** 2120–2124.
23. Maddox, P. S., Bloom, K. S. & Salmon, E. D. (2000) *Nat. Cell Biol.* **2,** 36–41.
24. Winey, M., Mamay, C. L., O'Toole, E. T., Mastronarde, D. N., Giddings, T. H., Jr., McDonald, K. L. & McIntosh, J. R. (1995) *J. Cell Biol.* **129,** 1601–1615.
25. Zeng, X., Kahana, J. A., Silver, P. A., Morphew, M. K., McIntosh, J. R., Fitch, I. T., Carbon, J. & Saunders, W. S. (1999) *J. Cell Biol.* **146,** 415–425.
26. Wolfe, B. A. & Gould, K. L. (2005) *Trends Cell Biol.* **15,** 10–18.
27. DeMarini, D. J., Adams, A. E., Fares, H., De Virgilio, C., Valle, G., Chuang, J. S. & Pringle, J. R. (1997) *J. Cell Biol.* **139,** 75–93.
28. Dobbelaere, J. & Barral, Y. (2004) *Science* **305,** 393–396.
29. Muller-Reichert, T., Sassoon, I., O'Toole, E., Romao, M., Ashford, A. J., Hyman, A. A. & Antony, C. (2003) *Chromosoma* **111,** 417–428.
30. Longtine, M. S., McKenzie, A., III, Demarini, D. J., Shah, N. G., Wach, A., Brachat, A., Philippsen, P. & Pringle, J. R. (1998) *Yeast* **14,** 953–961.
31. Pearson, C. G., Maddox, P. S., Zarzar, T. R., Salmon, E. D. & Bloom, K. (2003) *Mol. Biol. Cell* **14,** 4181–4195.
32. Shaw, S. L., Yeh, E., Bloom, K. & Salmon, E. D. (1997) *Curr. Biol.* **7,** 701–704.
33. Pringle, J. R. & Mor, J. R. (1975) *Methods Cell Biol.* **11,** 131–168.
34. Bi, E., Maddox, P., Lew, D. J., Salmon, E. D., McMillan, J. N., Yeh, E. & Pringle, J. R. (1998) *J. Cell Biol.* **142,** 1301–1312.
35. Meluh, P. B., Yang, P., Glowczewski, L., Koshland, D. & Smith, M. M. (1998) *Cell* **94,** 607–613.
36. McCleland, M. L., Gardner, R. D., Kallio, M. J., Daum, J. R., Gorbsky, G. J., Burke, D. J. & Stukenberg, P. T. (2003) *Genes Dev.* **17,** 101–114.
37. Pearson, C. G., Yeh, E., Gardner, M., Odde, D., Salmon, E. D. & Bloom, K. (2004) *Curr. Biol.* **14,** 1962–1967.
38. Cooke, C. A., Heck, M. M. & Earnshaw, W. C. (1987) *J. Cell Biol.* **105,** 2053–2067.
39. Goh, P. Y. & Kilmartin, J. V. (1993) *J. Cell Biol.* **121,** 503–512.
40. Carminati, J. L. & Stearns, T. (1997) *J. Cell Biol.* **138,** 629–641.
41. Tirnauer, J. S., O'Toole, E., Berrueta, L., Bierer, B. E. & Pellman, D. (1999) *J. Cell Biol.* **145,** 993–1007.
42. Sorger, P. K., Severin, F. F. & Hyman, A. A. (1994) *J. Cell Biol.* **127,** 995–1008.
43. Yoon, H. J. & Carbon, J. (1999) *Proc. Natl. Acad. Sci. USA* **96,** 13208–13213.
44. Russell, I. D., Grancell, A. S. & Sorger, P. K. (1999) *J. Cell Biol.* **145,** 933–950.
45. Higuchi, T. & Uhlmann, F. (2005) *Nature* **433,** 171–176.
46. Granot, D. & Snyder, M. (1991) *Cell Motil. Cytoskeleton* **20,** 47–54.
47. Hoyt, M. A., Totis, L. & Roberts, B. T. (1991) *Cell* **66,** 507–517.
48. Li, R. & Murray, A. W. (1991) *Cell* **66,** 519–531.
49. Fraschini, R., Beretta, A., Lucchini, G. & Piatti, S. (2001) *Mol. Genet. Genomics* **266,** 115–125.
50. Canman, J. C., Cameron, L. A., Maddox, P. S., Straight, A., Tirnauer, J. S., Mitchison, T. J., Fang, G., Kapoor, T. M. & Salmon, E. D. (2003) *Nature* **424,** 1074–1078.
51. McCarroll, R. M. & Fangman, W. L. (1988) *Cell* **54,** 505–513.